POTASSIC MAGMATISM FROM CENTRAL-EASTERN PARAGUAY: PETROGENESIS AND GEODYNAMIC INFERENCES

P.Comin-Chiaramonti, A.Cundari, A.De Min, C.B.Gomes, E.M.Piccirillo

Alkaline Magmatism in Central-Eastern Paraguay. Relationships with Coeval Magmatism in Brazil. Comin-Chiaramonti, P. & Gomes, C. B. (eds.), 1996, Edusp/Fapesp, São Paulo, pp. 207-222.

ABSTRACT

Potassic magmas, emplaced in the Asunción-Sapucai graben (ASU) between 132 and 118 Ma ago, are represented by two main suites, i.e. basanite-tephrite-phonotephrite-phonolite and alkali basalt-trachybasalt-trachyandesite-trachyphonolite/trachyte. The compositional variations indicate fractional crystallization processes, along with mainly olivine+clinopyroxene accumulation and mixing between magmas of varying degrees of evolution. The primary magmas are inferred to have 12-13% MgO and to have been generated from about 3% melting of a garnet peridotite which suffered variable enrichment in incompatible elements with respect to the primordial mantle. In the Asunción-Sapucai graben are present tholeiitic stratoid volcanics (137-130 Ma) and sodic rock-types (61-39 Ma), also referred to garnet mantle sources. The geochemical systematics and constraints for the whole magmatism from the Eastern Paraguay show a generalized lithospheric source, variously metasomatized, which suffered various degrees of partial melting and where compositional heterogeneities were preserved up to Oligocene times. The generalized situation severely constraints any interpretation of the Dupal anomaly inside the continent (Hawkesworth et al., 1986) and current interpretation relative to the Tristan da Cunha plume.

INTRODUCTION

Volcanic/subvolcanic potassic suites are widespread in central-eastern Paraguay, mainly in the Asunción-Sapucai graben (ASU), an extensional structure that experienced intense magmatic activity since Early Cretaceous. The magmatic events started with the emission of flood tholeiites of the Alto Paraná Formation (i.e. Serra Geral Formation in Brazil) at 137-130 Ma (Bitschene, 1987; Turner et al., 1994; Ernesto et al., this volume), followed by potassic complexes and dykes at about 128 Ma (Gomes et al., this volume); the late stages (61-39 Ma: Comin-Chiaramonti et al., 1991) display a distinctive sodic character.

The ASU potassic magmatism forms shallow-level intrusive complexes overlain by lava-flows crosscut by a large number of dykes (Comin-Chiaramonti et al., this volume, Appendix I). Notably, the intrusive facies and lava flows have compositions similar to those of the

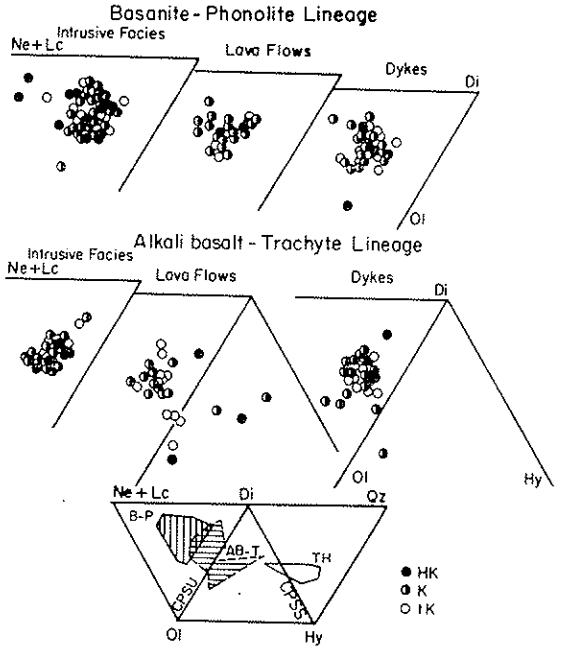

Figure 1 - Distribution of {SiO_2 < 52.5 wt %; mg# MgO/(MgO+FeO) > 0.50} in the normative basalt tetrahedron (Yoder & Tilley, 1962). Inset: B-P and AB-T variation fields compared with the field of the stratoid tholeiitic volcanics (TH) from central-eastern Paraguay (data source: Bellieni et al., 1986; Comin-Chiaramonti et al., this volume, Appendix II). CPSU and CPSS: critical planes of silica-undersaturation and saturation, respectively.

dykes, so that the latter can be considered the potential feeder of the ASU potassic magmatism.

The geochemical variations are quite irregular, showing the scatter typical of open-system processes (Comin-Chiaramonti et al., this volume, Petrochemistry). On the whole, the ASU potassic rock-types display characteristics typical of the RPT group of Barton (1979), i.e. "plagioleucitite" group of Foley (1992).

Two main suites are apparent: basanite to phonolite (B-P) and alkali basalt to trachyphonolite/trachyte (AB-T), both characterized by variable K_2O/Na_2O ratios. The latter allows to distinguish highly potassic (HK), potassic (K) and transitional potassic (tK) groups within each suite (cf. Comin-Chiaramonti et al., this volume, Magmatism).

Notably, the AB-T suite is less silica-undersaturated than the B-P one and the former displays lower TiO_2, K_2O, Zr, Nb, Y and REE contents (Comin-Chiaramonti et al., this volume, Petrochemistry).

Yoder & Tilley (1962) tetrahedron (Fig. 1) highlights the distinction between the silica-undersaturated compositions of the B-P suite and those of the AB-T suite, which are both silica-undersaturated and silica-saturated, and sometimes straddle the critical plane of silica-undersaturation . The normative domains of the two suites are not a simple function of the K_2O/Na_2O ratio, as HK, K and tK compositions lie at both ends of the trends. Moreover, the AB-T suite does not satisfy a simple fractionation process as compositions with relatively high mg# plot at both ends of the field. The latter may imply mixing between silica-undersaturated and silica-saturated magmas, or may represent magmas produced by variable degrees of partial melting, or both.

PROCESSES POSSIBLY INVOLVED IN THE EVOLUTION OF ASU MAGMAS

Crystal fractionation

Modelling of crystal fractionation involving ten major oxide components was performed on each complex and on selected samples (cf. Comin-Chiaramonti et al., 1990; Marzoli, 1991; Comin-Chiaramonti et al., 1992; De Min, 1993), using the least squares program XLFRAC (Stormer & Nichols, 1978).

Models with low sums of the square residuals ($\Sigma R^2 < 0.5$) relative to the AB-T suite (i.e. alkali basalt-trachybasalt-trachyandesite-trachyphonolite/trachyte) indicate that the most evolved alkali basalts, trachybasalts and trachyphonolites could be the products of crystal fractionation of olivine+clinopyroxene+magnetite±plagioclase±biotite. The trace element modelling (Rayleigh's equation) show that incompatible elements have observed/calculated ratios mainly in the range 0.70-1.30.

The same approach for the B-P suite (i.e. basanite-tephrite-phonotephrite-phonolite) shows that the dominant fractionating assemblages are olivine+clinopyroxene+magnetite± biotite±plagioclase±leucite ($\Sigma R^2 = 0.10$-1.95), with variable SiO_2 depletions and enrichments in the residual liquids which evolved in the Mg_2SiO_4 - $KAlSiO_4$ - SiO_2 - H_2O volume (cf. Hamilton & MacKenzie, 1965; Luth, 1967), as also indicated by mineralogical features (cf.

Table 1 - Major (wt %) and trace (ppm) element average contents, relative standard deviations (s.d.) of ASU magmas. B-P suite: B, basanite; T, tephrite; PT, phonotephrite; P, phonolite. AB-T suite: AB, alkali basalt; TB, trachybasalt; TA, trachyandesite; TP, trachyphonolite; TR, trachyte. N = number of samples, mg# = atomic Mg/(Mg+Fe²⁺), assuming Fe³⁺/Fe²⁺ ratio = 0.18.

B-P suite

	B	s.d.	T	s.d.	PT	s.d.	P	s.d.
	(N=3)		(N=74)		(N=101)		(N=23)	
SiO_2	48.86	(0.34)	49.36	(1.21)	50.85	(1.47)	54.28	(2.49)
TiO_2	1.55	(0.12)	1.79	(0.25)	1.65	(0.25)	1.04	(0.40)
Al_2O_3	13.30	(0.25)	15.17	(1.69)	16.68	(1.49)	19.48	(1.07)
FeO_t	9.33	(0.95)	9.60	(0.82)	8.67	(1.03)	5.41	(1.65)
MnO	0.17	(0.01)	0.17	(0.02)	0.17	(0.02)	0.15	(0.03)
MgO	8.54	(1.50)	6.25	(1.19)	4.44	(0.98)	1.56	(1.07)
CaO	10.86	(0.93)	9.26	(0.89)	7.54	(0.97)	4.63	(1.51)
Na_2O	3.40	(0.21)	3.33	(0.61)	4.02	(0.60)	6.05	(1.39)
K_2O	3.53	(0.60)	4.48	(0.88)	5.37	(1.12)	7.00	(1.14)
P_2O_5	0.46	(0.08)	0.59	(0.17)	0.61	(0.16)	0.40	(0.26)
mg#	0.65		0.57		0.51		0.37	
Cr	388	(15)	161	(111)	70	(65)	16	(16)
Ni	140	(40)	51	(27)	34	(20)	6	(5)
Ba	1214	(4)	1470	(336)	1563	(357)	2022	(1104)
Rb	61	(20)	90	(28)	107	(37)	129	(39)
Sr	1383	(150)	1703	(323)	1731	(441)	2443	(719)
La	73	(13)	85	(22)	97	(23)	126	(36)
Ce	136	(27)	153	(36)	171	(39)	205	(47)
Nd	58	(3)	67	(14)	76	(28)	84	(18)
Zr	162	(36)	258	(74)	299	(72)	531	(150)
Y	18	(4)	20	(5)	21	(5)	25	(9)
Nb	38	(7)	40	(12)	48	(15)	77	(21)

AB-T suite

	AB	s.d.	TB	s.d.	TA	s.d.	TP	s.d.	TR	s.d.
	(N=8)		(N=52)		(N=65)		(N=20)		(N=15)	
SiO_2	50.72	(1.74)	51.43	(1.17)	53.53	(1.97)	58.58	(2.39)	60.91	(2.45)
TiO_2	1.53	(0.27)	1.51	(0.22)	1.50	(0.23)	0.83	(0.43)	0.94	(0.44)
Al_2O_3	12.99	(1.73)	15.62	(1.62)	17.20	(1.36)	19.04	(0.90)	18.24	(0.84)
FeO_t	9.11	(1.38)	8.75	(0.61)	7.88	(1.24)	4..22	(1.74)	4.26	(1.70)
MnO	0.17	(0.03)	0.16	(0.02)	0.15	(0.02)	0.14	(0.04)	0.12	(0.10)
MgO	8.63	(1.44)	6.04	(1.45)	3.84	(1.27)	1.14	(0.81)	1.34	(0.73)
CaO	9.86	(0.79)	8.46	(0.74)	6.34	(1.22)	3.47	(1.31)	2.28	(1.54)
Na_2O	2.60	(1.19)	3.31	(0.67)	3.76	(0.90)	5.60	(1.21)	4.21	(1.02)
K_2O	3.93	(1.05)	4.24	(1.07)	5.27	(1.44)	6.71	(0.93)	7.43	(1.86)
P_2O_5	0.46	(0.09)	0.49	(0.11)	0.55	(0.11)	0.27	(0.19)	0.31	(0.18)
mg#	0.66		0.59		0.50		0.36		0.39	
Cr	316	(86)	165	(143)	64	(48)	8	(10)	10	(13)
Ni	91	(33)	59	(36)	24	(21)	6	(5)	8	(5)
Ba	1444	(344)	1310	(265)	1417	(376)	1334	(811)	1140	(482)
Rb	77	(35)	89	(28)	104	(32)	131	(34)	136	(32)
Sr	1251	(185)	1496	(288)	1440	(353)	1358	(692)	815	(325)
La	65	(38)	72	(18)	87	(22)	114	(36)	93	(39)
Ce	124	(58)	126	(32)	153	(34)	185	(59)	159	(62)
Nd	52	(19)	53	(12)	66	(15)	64	(25)	64	(28)
Zr	210	(90)	224	(52)	295	(54)	541	(167)	440	(130)
Y	18	(5)	19	(4)	21	(4)	22	(10)	22	(10)
Nb	29	(14)	31	(8)	40	(9)	66	(26)	50	(23)

Table 2 - Mineral compositions used in mass balance calculations, B-P and AB-T suites. Ol, olivine; Cpx, clinopyroxene, Biot, biotite; Amph, amphibole; Mt, magnetite; Pl, plagioclase; Af, alkali feldspar; Lc, leucite; Ap, apatite. Other abbreviations as in Table 1 (data source: Comin-Chiaramonti et al., this volume, Appendix III).

B-P suite

	Ol B	Ol T	Ol PT	Cpx B	Cpx T	Cpx PT	Biot B	Biot T	Biot PT	Mt B	Mt T	Mt PT	Pl B	Pl T	Pl PT	Lc T	Lc PT	Ap T	Ap PT
SiO_2	39.98	39.12	38.43	52.16	51.80	47.74	39.87	40.03	37.69	0.19	0.23	0.80	50.99	53.50	59.87	55.28	54.72	0.32	
TiO_2				1.09	0.98	1.42	6.02	8.98	6.29	23.93	18.19	18.23							
Al_2O_3				2.25	2.33	5.66	15.46	12.48	16.29	3.95	5.43	4.02	30.96	29.78	24.71	23.33	22.97	0.09	
FeO_t	14.33	18.57	22.29	5.85	7.15	7.73	11.50	12.47	14.60	68.78	73.74	75.71	0.37	0.18	0.24	0.19	0.50	0.37	1.59
MnO	0.26	0.37	0.51	0.10	0.19	0.18	0.12	0.12	0.12	0.56	1.03	0.85	0.01	0.01				0.04	0.22
MgO	45.23	41.69	38.53	16.20	15.48	12.42	18.29	15.69	14.90	2.56	1.32	0.34	0.27	0.01				0.01	0.56
CaO	0.24	0.25	0.24	22.28	21.63	24.43	0.01	0.01	0.01	0.07	0.05	0.05	13.92	11.89	6.74	0.24	0.08	55.89	54.78
Na_2O				0.07	0.43	0.42	0.13	0.96	9.23				3.29	4.45	6.70	1.29	0.66	0.10	
K_2O					0.01	0.01	8.60	9.27	9.86				0.13	0.18	1.73	19.67	21.06	0.01	
P_2O_5																		43.17	42.84

AB-T suite

	Ol AB	Ol TB	Ol TA	Cpx AB	Cpx TB	Cpx TA	Biot AB	Biot TB	Biot TA	Amph TA	Mt AB	Mt TB	Mt TA	Pl TB	Pl TA	Af TA	Ap TA
SiO_2	39.98	39.43	38.42	49.57	51.00	51.39	39.92	40.12	38.11	41.54	0.16	0.12	0.05	48.79	54.71	65.25	0.16
TiO_2				1.70	1.33	1.25	8.23	6.97	7.88	4.64	17.33	24.14	19.26				
Al_2O_3				4.99	3.03	3.02	12.84	13.88	14.81	11.87	3.41	2.81	2.27	32.85	28.85	19.24	0.05
FeO_t	14.30	16.92	22.40	5.56	7.09	7.72	12.77	12.53	12.87	13.13	75.55	69.50	76.29		0.18	0.72	0.98
MnO	0.25	0.55	0.32	0.28	0.30	0.39	0.11	0.21	0.26	0.37	1.01	1.10	1.29				0.13
MgO	45.47	42.99	38.70	16.69	15.44	14.27	16.03	17.08	15.40	11.52	2.39	2.23	0.84				0.28
CaO		0.11	0.16	20.79	21.25	21.65	0.01	0.01	0.15	12.32	0.15	0.09		15.69	10.83	0.64	55.43
Na_2O				0.42	0.54	0.30	0.36	0.01	0.27	2.69				2.49	5.26	5.5	0.05
K_2O				0.01	0.01	0.01	9.73	9.21	10.24	1.94				0.18	0.17	8.65	
P_2O_5																	42.93

Table 3 - Fractionation models. Least square mass balance calculations based on major elements (Stormer & Nicholls, 1978). Abbreviations as in Tables 1 and 2. F: weight fraction of daughter liquid at each stage. The numbers are the amounts (wt %) of minerals subtracted from the parent to obtain the daughter magma. ΣR^2: sum of the square residuals.

	B-P suite						AB-T suite								
Parent magma	B 1	B 2	B 3	T	PT 1	PT 2	AB 2	AB 2	TB 1	TB 2	TA 1	TA 2	TA 3	TA 1	TA 2
Derived liquid	T	T	T	PT	P	P	TB	TB	TA	TA	TP	TP	TP	TR	TR
F%	82.69	84.42	78.92	72.56	42.49	58.19	80.86	81.48	77.46	75.20	66.80	70.03	73.01	52.34	53.18
Ol	14.86	16.31		1.80	8.71		14.17	15.97	12.15		4.86	11.38		4.46	
Cpx	74.00	80.94	73.86	49.62	30.32	46.49	78.56	79.92	53.70	57.30	33.95	27.18	37.27	7.50	11.96
Biot			18.91	13.06		20.14	3.58			17.17	15.56		20.78		6.09
Amph												13.31		31.88	31.85
Mt	1.58	2.74	1.78	8.48	9.29	8.90	3.69	4.11	8.35	6.59	11.54	12.68	11.13	7.43	7.30
Pl	9.56		5.45	22.46	34.66	21.57			25.80	18.93	32.36	32.49	29.96	29.66	28.61
Af														16.18	12.12
Lc				3.81	16.08	2.90									
Ap				0.76	0.93						1.73	2.95	0.87	2.88	2.08
ΣR^2	0.545	0.725	0.970	0.155	0.007	1.776	0.649	0.655	0.153	0.428	0.645	0.974	0.730	0.430	0.541

Table 4 - Mineral/liquid partition coefficients (source data in Caroff et al., 1993 and therein references; Marzoli, 1991 and therein references). Abbreviations as in Table 2.

	Ol	Cpx	Biot	Amph	Mt	Pl	Af	Lc	Ap
Cr	0.72	5.69	1.00	8.00	7.70	0.03	0.01	0.06	0.01
Ni	30.71	2.00	8.00	6.40	6.54	0.03	0.01	0.06	0.01
Ba	0.04	0.07	10.00	0.61	0.14	0.24	3.02	0.18	0.95
Rb	0.08	0.10	3.00	0.15	0.23	0.03	0.42	0.44	0.56
Sr	0.01	0.33	0.20	1.01	0.23	2.12	4.11	0.02	1.67
La	0.01	0.22	0.02	0.56	0.53	0.12	0.46	0.02	5.16
Ce	0.01	0.34	0.02	0.87	0.56	0.14	0.36	0.02	6.34
Nd	0.01	0.68	0.03	1.82	0.55	0.07	0.31	0.02	6.60
Zr	0.05	0.10	0.08	0.80	0.35	0.01	0.13	0.01	0.01
Y	0.01	0.77	0.80	2.88	0.55	0.05	0.24	0.01	5.08
Nb	0.01	0.14	0.30	0.89	3.86	0.01	0.12	0.02	0.09

Table 5 - Trace elements: observed/ calculated ratios (Rayleigh fractionation, $C^i_L = C^i_O\ F^{(Di-1)}$ where C^i_L = concentration of trace element i in the liquid; C^i_O = concentration of trace element i in the parental magma; F = weight proportion of residual liquid; Di = bulk partition coefficient for element i for the crystal settling out of the melt). Abbreviations as in Table 3.

	B-P suite						AB-T suite								
	T (1)	T (2)	T (3)	PT	P (1)	P (2)	TB (1)	TB (2)	TA (1)	TA (2)	TP (1)	TP (2)	TP (3)	TR (1)	TR (2)
Cr	0.80	0.81	0.96	1.02	0.73	0.76	1.20	1.18	0.79	0.90	0.29	032	0.25	0.84	0.95
Ni	0.97	0.98	0.55	1.21	1.20	0.50	1.34	1.39	1.87	1.07	0.90	1.35	0.50	2.41	1.38
Ba	1.02	0.97	1.52	1.21	0.69	2.18	0.80	0.75	0.86	1.36	1.24	0.72	1.37	0.70	1.56
Rb	1.24	1.27	1.36	1.01	0.64	1.02	0.98	0.96	0.93	1.04	1.05	0.92	1.33	0.76	0.91
Sr	1.11	1.09	1.07	0.93	1.29	1.20	1.03	1.03	0.90	0.86	0.90	0.93	0.90	0.90	0.79
La	1.00	1.02	0.96	0.91	0.72	0.84	0.93	0.94	0.99	0.96	0.98	1.08	1.03	0.77	0.75
Ce	0.98	1.00	0.95	0.93	0.69	0.84	0.87	0.88	1.01	0.98	0.93	1.01	0.97	0.82	0.79
Nd	1.05	1.07	1.12	0.98	0.68	0.81	0.93	0.93	1.08	1.06	0.77	0.88	0.80	0.93	0.91
Zr	1.34	1.37	1.29	0.87	0.89	1.14	0.88	0.89	1.04	1.02	1.27	1.37	1.38	0.96	0.97
Y	1.03	1.05	1.05	0.94	0.74	0.82	1.00	1.00	0.97	1.00	0.88	0.99	0.92	1.20	1.22
Nb	0.90	0.92	0.88	1.00	1.03	1.25	0.91	0.92	1.11	1.08	1.37	1.46	1.43	0.97	0.98

Cundari & Comin-Chiaramonti, this volume). This is also consistent with different fO_2 and H_2O regimes, expanding the biotite volume and suppressing leucite at relatively low pressure.

Considering the ASU sampling as statistically representative of the erupted magmas, an attempt to simplify the question relative to the crystal fractionation in terms of averages of the main petrographical/petrochemical types is presented (i.e. considering on the whole the intrusive facies + lava flows + dykes as a roughly closed system; cf. Schiano et al., 1993). Average compositions of the magma types and representative compositions of their phenocrysts are presented in Tables 1 and 2, respectively, and the modellization results (major elements) are shown in Table 3.

B-P suite. The starting composition (basanite) displays various possible solutions to obtain tephrite (sums of square residues lower than unity) with fractionating assemblages ranging from 21.0 to 15.6 wt % (clinopyroxene + magnetite ± olivine ± biotite ± plagioclase). Phonotephrite is obtained from tephritic liquid fractionating 27.5 wt % of olivine + clinopyroxene + magnetite + biotite + plagioclase+leucite+apatite. The best solution to obtain phonolite is represented by 57.5 wt % solid fractionate in phonotephritic liquid (olivine +clinopyroxene + magnetite + plagioclase +leucite + apatite).

The observed/calculated ratios of trace elements (mineral/liquid partition coefficients in Table 4) display ranges between 0.8 and 1.4, Ni and Ba of phonolite excepted (1.2 to 0.5 and 0.7 to 2.3, respectively; cf. Table 5). Notably, the scatters are in the range of standard deviations of the average rock-types.

AB-T suite. The fractionating assemblages are around 20 wt % for trachybasalt from alkali basalt (olivine+clinopyroxene+magnetite± biotite); 22-25 wt % for trachyandesite from trachybasalt (olivine+clinopyroxene+ magnetite+plagioclase±biotite); 27-33 wt % for trachyphonolite from trachyandesite (clinopyroxene+plagioclase+magnetite+apatite± biotite±amphibole).

Trachyte is derived from trachyandesite by fractionating 57-58 wt % of clinopyroxene+ magnetite+amphibole+plagioclase+alkali feldspar+apatite±olivine±biotite. Notably, significant amphibole fractionation (up to 17%) may explain the transition from ol-normative to Q-normative liquids (i.e. trachyandesite-trachyte transition).

The observed/calculated ratios relative to the trace elements (Table 5) are mainly in the range 0.8-1.2, excepting the scatters of Ni, Ba, Zr and Nb, above all in the more evolved rock-types.

On the whole, it is apparent that the fractional crystallization is an important process in the evolution of ASU magmas. However, although the scattering of observed/calculated ratios of the trace elements may reflect also variations on mineral/liquid distribution coefficients, other processes can be inferred from the petrographical and mineralogical evidences.

Previous studies of ASU alkaline rocks have stressed that the complexity of petrographical, mineralogical and geochemical changes in both B-P and AB-T suites is indicative of a complex genetic typology, other than fractional crystallization, e.g. olivine+ clinopyroxene±foids±feldspars±phlogopite accumulation, crystal/ liquid mixing from distinct magma batches, variations of O_2 and H_2O activities, leucite breakdown into pseudoleucite and/or analcimitization at low pressure regimes, exsolving CO_2-rich liquids (Comin-Chiaramonti et al., 1992; Cundari & Comin-Chiaramonti, this volume; Castorina et al., this volume, Carbonatites). However, the evolution history of ASU magmas remained largely within the stability fields of ferromagnesian phases, notably olivine+clinopyroxene, in the system Mg_2SiO_4-$KAlSiO_4$-SiO_2 (cf. Edgar, 1980), suggesting that a relatively high temperature subvolcanic regime prevailed in the evolution of the ASU magmas. The extreme differentiates from both B-P and AB-T suites approach the composition of peralkaline residua, suggesting an extended subvolcanic crystallization of K-rich, aluminous phases like biotite and/or leucite. The widespread occurrence of megacryst, probably xenocryst phases, points to crystal/liquid mixing from chemically distinct magma batches during their ascent to the surface (cf. Cundari & Comin-Chiaramonti, this volume).

Crystal accumulation and crystal/liquid mixing

Petrographical evidences show that the ASU magmas were subjected to varying degrees of crystal accumulation and to variable degrees of mixing between magmas containing higher- and lower-temperature assemblages (cf. Cundari & Comin-Chiaramonti, this volume). This complex situation is summarized in Figure 2, in terms of olivine-bulk rock relationships. The liquid products of crystal fractionation lie along a trend parallel to, but below, the Roeder-Emslie equilibrium curve. The xenocryst vector represents the situation where high-temperature olivine is preserved in lower-temperature magma by non-equilibration with the host liquid.

Olivine accumulation produces MgO-rich magmas in which olivine is less magnesian than the equilibrium olivine for that bulk composition. Magma mixing results in a range of phenocryst/

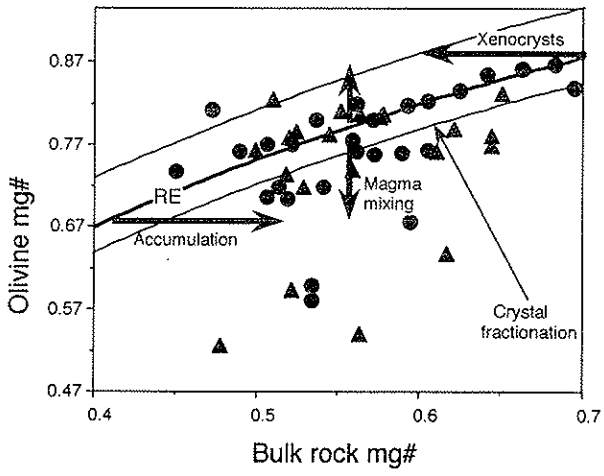

Figure 2 - Compositions of olivine phenocryst and microphenocryst cores plotted against bulk-rock compositions to show the effects of crystal fractionation, xenocrystal retention, magma mixing and olivine accumulation on the range of phenocrysts in individual specimens (cf. Cundari & Comin-Chiaramonti, this volume, Fig. 3). Arrows indicate direction of spread of olivine compositions resulting from the various processes. Circles and triangles: B-P and AB-T suites, respectively. RE, Roeder & Emslie (1970) equilibrium curve.

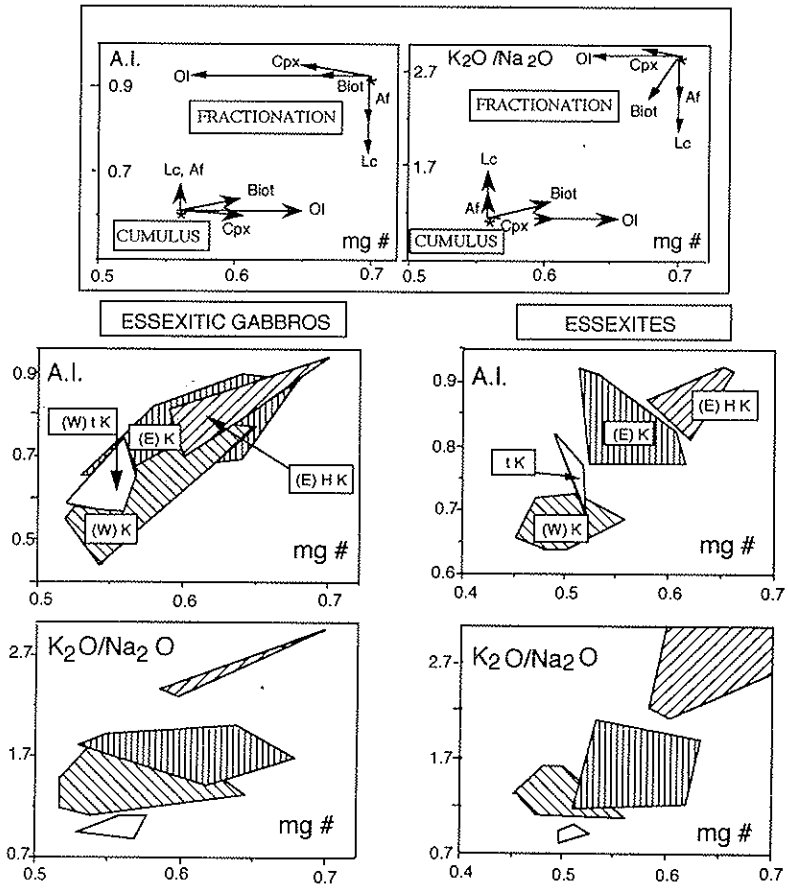

Figure 3 - Relationships between mg# and alkali index (A.I.) and K_2O/Na_2O ratio (wt %) for ASU essexitic gabbros and essexites. HK, K, tK: high potassic, potassic and transitional potassic rock-types, respectively. (E) and (W): eastern and western region, respectively. Insect: vectors (proportional intensities) representative of fractionation and cumulus processes (whole-rocks and minerals from Comin-Chiaramonti et al., Appendices II and III). Ol, Olivine; Cpx, clinopyroxene; Biot, biotite; Af, alkali feldspar; Lc, leucite.

microphenocryst core compositions, which can be either more or less magnesian than the equilibrium olivine composition.

Regarding the intrusive facies, e.g., essexitic gabbros and essexites, there are positive relationships between mg# and alkali index and between mg# and K_2O/Na_2O ratios, displaying large overlap for the two clans and internal evolution driven by fractionation and cumulus of potassic phases as biotite, leucite and/or alkali feldspar, other than olivine and clinopyroxene (Fig. 3).

In the AB-T suites two distinct megacryst generations were observed, i.e. diopside and salite with (Si+Al) < 2.00 and > 2.00 a.f.u., corresponding to Ti/Al = 4.0 and 0.11, respectively. The former megacrysts probably crystallized from liquid compositions with (Na+K)/Al > 1 (Comin-Chiaramonti et al., 1990). Notably, close chemical correlations apply only to the olivine-clinopyroxene pairs from B-P suite, reflecting their cognate relationships, whereas there is poor correlation for $Fe_t/(Fe_t+Mg)$ values between coexisting olivine and clinopyroxene compositions in AB-T suites (Comin-Chiaramonti et al., 1990, 1992).

Variations of Oxygen fugacity

The evidences of fO_2 variations are inferred from the mineralogical characteristics (Comin-Chiaramonti et al., 1990, 1992; Cundari & Comin-Chiaramonti, this volume), e.g.:

1) Magnetite-ilmenite pairs generally indicate temperatures and fO_2 conditions between MW and NNO buffers, both in B-P and AB-T suites, up to phonolitic/trachyphonolitic rock-types where the conditions shift towards the H-M buffer. Moreover, ilmenite exsolutions in magnetite hosts of some intrusive facies testify equilibration down to very low temperatures and fO_2 (i.e. < 400°C and < -30, respectively).

2) Biotite microlites from the AB-T suite fall close to H-M buffer in the Mg-Fe^{2+}-Fe^{3+} system of Wones & Eugster (1965). In comparison biotite from the B-P suite is removed from the region of buffered compositions, suggesting that the mica crystallization in the corresponding liquids occurred under unbuffered oxigen conditions.

3) Olivine and magnetite may disappear at phonotephrite/phonolite transition, and they are replaced by andradite and haematite in the B-P suite.

Test of open-system model

The fact that the evolution of ASU suites can be modelled by the Rayleigh's equation means that they have evolved either by roughly closed-system fractional crystallization, or following open-system fractionation. In the latter model, fractional crystallization occurs in the magmatic chambers together with cyclic replenishment and only partial extraction of the differentiated liquid during each cycle (open-system fractionation in a periodically replenished magma chamber: PRF, cf. O'Hara & Mathews, 1981). The chambers are filled up by batches of fresh magma which mixes with residual liquids from previous cycles. This mixed liquid evolves according to the Rayleigh's law and part of the residual liquid is expelled through eruption at the end of the cycle. This model is described by equation (O'Hara & Mathews, 1981): $Y = \{(1-X)^{(Di-1)} (X (1-E)+E)-E\}/\{(1-X)^{(Di-1)} (E-1)\}$, where E is C^i_L/C^i_O ratio (C^i_L concentration of trace element "i" in the erupted liquid; C^i_O, concentration of "i" in the fresh magma), X and Y are the fraction of liquid crystallized and erupted at each cycle, respectively.

The above equation has been used to model the behaviour of incompatible (Th and Zr) and compatible (Cr and Ni) elements in the B-P and AB-T suites, basanite to tephrite and alkali basalt to trachybasalt, respectively.

The results are shown as curves on the Y vs. X diagram, relative to basanite-tephrite and alkali basalt-trachybasalt (Fig. 4). Theoretically the curves should intersect for the right Y and X val-

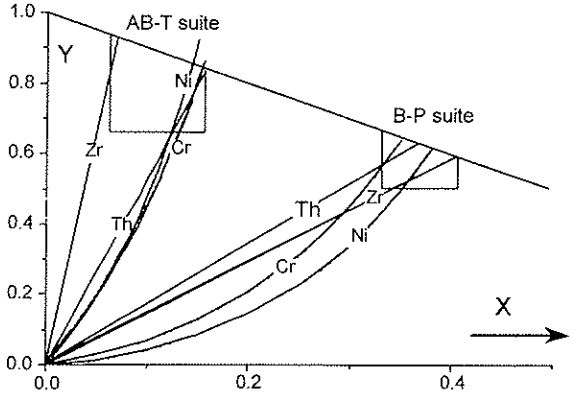

Figure 4 - X vs. Y diagram (O'Hara & Mathews, 1981). B-P suite (basanite-tephrite): C^i_L/C^i_O Cr = 0.415; Ni = 0.364; Zr = 1.592; Th = 1.511; D_{bulk}: Cr = 3.030; Ni = 3.108; Zr = 0.096; Th = 0.102. AB-T suite (alkali basalt-trachybasalt): C^i_L/C^i_O Cr = 0.522; Ni = 0.429; Zr = 1.067; Th = 1.150; D_{bulk}: Cr = 4.905; Ni = 6.451; Zr = 0.101; Th = 0.184.

ues. However, because of the uncertainties on the utilized chemical parameters, we consider a good fitting the case of B-P suite, where all the curves intersect within the box defined at X = 0.35±0.05 and Y = 0.57±0.13. Although the corresponding intersects relative to AB-T suite are more scattered, the curves relative to the compatible and incompatible elements tend to converge near the X+Y = 1 line (box X = 0.10±0.05 and Y = 0.85±0.15). In both cases, the sum of X+Y is close to unity, which indicates that PRF model is roughly equivalent to a succession of closed-system fractionation events. The same approach relative to tephrite-phonotephrite and trachybasalt-trachyandesite yields similar results. On the contrary, calculations performed on the phonotephrite-phonolite and trachyandesite-trachyphonolite/trachyte yield negative values for Cr and Ni. Consequently, the behaviour of trace elements is controlled by Rayleigh's law at least up to phonotephritic/trachyandesitic magmas. The more evolved rock-types (i.e. phonolites and trachyphonolites/trachytes), probably reflect the drastic changes in fO_2 and in crystal/liquid elemental partition coefficients, other than a major chemical reactivity at low temperature/weathering processes (i.e. analcitization, zeolitization and so on).

SOURCE CHARACTERISTICS

On the whole, the chemical signature of possible parental, i.e. primary magma(s) is difficult to establish because of the processes involved in magma differentiation at shallow depth and subsolidus transformations (see also Comin-Chiaramonti et al., this volume, Magmatism and Petrochemistry; Cundari & Comin-Chiaramonti, this volume).

In general the more magnesian ASU rock-types do not satisfy the commonly accepted criteria for primary magmas, i.e. mg# Mg/(Mg + Fe^{2+}) > 0.65 and Ni contents > 235 ppm (cf. Sato, 1977; Frey et al., 1978), and even those rock-types where mg# is in the range of primitive mantle-derived magmas the Ni contents are in the range between 66 and 154 ppm.

Assuming that the least evolved compositions (cf. basanite and alkali basalt rock-types of Table 1) represent derivative liquids, we need to consider compositions with relatively high mg#, e.g. between 0.74 and 0.76 (Fo around 0.90 for equilibrium olivine). Possible compositions are obtained by adding c.23 wt % clinopyroxene + olivine (clinopyroxene 61.4 %; olivine 38.6 %) and 21.5 wt % (clinopyroxene 68.6 %; olivine 31.4 %) to basanite (mg# 0.65) and to alkali basalt (mg# 0.66) of Table 1, respectively. The results are summarized in Table 6.

Assuming a garnet peridotite as mantle source (cf. Comin-Chiaramonti et al., 1991, 1992), for the low yttrium contents of the observed and calculated concentrations, for the strong fractionation of the HREE (Comin-Chiaramonti et al., this volume, Petrochemistry) and because spinel peridotite sources indicate melting degrees less than 1.5 %, the models show melting degrees around 3.2 % for both basanite and alkali basalt parent magmas (Table 6). The models also show residual garnet (4.1-4.5 wt %) ± amphibole (0.07 and 0.47 wt % B-P and AB-T, respectively) and important enrichments and depletions (Table 6 and Fig. 5) in the mantle source with respect to the primordial mantle of e.g. Sun & McDonough (1989).

Notably, garnet peridotite sources are also inferred by melting models for the Mesozoic tholeiitic basalts of the Alto Paraná/Serra Geral Formation (melting degrees: high-Ti basalts, 5-9%; low-Ti basalts, 20%; Piccirillo & Melfi, 1988) and for the Tertiary nephelinites of the Asunción area (melting degrees: 3-6%; Comin-Chiaramonti et al., 1991).

Incompatible element enrichment may be broadly associated with metasomatic processes involving fluids and/or small volume melts (cf. Menzies & Hawkesworth, 1987; Erlank et al., 1987). Whatever the origin of these fluids, the source was probably in the deeper parts of the lithosphere or upper asthenosphere and such fluids were likely derived from volatile-rich alkaline melts (cf. Castorina et al., this volume, Sr/Nd).

Different metasomatized sources can be envisaged by the occurrence in the Asunción-Sapucai graben of Na-(ultra)alkaline magmatism (61-39 Ma: La_N/Lu_N = 32.4) carrying spinel mantle xenoliths. The latter are not a suitable source for the associated magmatism (Comin-Chiaramonti et al., 1991, 1992), but the occur-

rence of two main suites, i.e. blebs-bearing (BB: strongly enriched in K and other incompatible elements) and bleb-free (BF: moderately enriched in K and I.E.) would involve mantle enrichment and heterogeneity on local scale (Comin-Chiaramonti et al., 1986; Demarchi et al., 1988) and could indicate a plausible means of mantle metasomatism on a small scale. The REE contents of clinopyroxenes from BB and BF mantle xenoliths from the same outcrop (Ñemby hill; cf. Demarchi et al., 1988) is in agreement with the above assumption. In particular, REE profiles show LREE enrichment of BB clinopyroxene in comparison with BF ones (Fig. 6).

GEODYNAMIC SIGNIFICANCE

The magmatism of the Asunción-Sapucai graben is an example of potassic volcanism in an intracontinental rifting. In general, Ba and Sr contents of the rock-types are high, as might be expected from the potassic character of the ASU suites. However, not all incompatible elements show enrichments: thus Nb is up to 62 ppm in some phonolites. As a result, the ratio of large ion lithophile elements patterns normalized to primordial mantle show strong LILE/HFSE fractionation and negative Ta, Nb, P, Zr, Ti spikes (Comin-Chiaramonti et al., this volume, Petrochemistry), interpreted by some (e.g. Edgar, 1980; Pearce, 1983; Thompson et al., 1984; Beccaluva et al., 1991) in terms of subduction-related processes.

Comin-Chiaramonti et al. (1992) stressed the close similarity of the ASU potassic magmatism with the generalized patterns of the Roman Region lavas (RRL), the latter interpreted as the result of a subduction-driven activity (cf. Civetta et al., 1987; Beccaluva et al., 1991). However, the K-alkaline magmatism occurs in Paraguay in a rifted continental setting devoid of any orogenic and/or subduction-driven activity. It is interesting to note that Nb-Ta-Ti negative anomalies are likewise shown in the same area by the coeval tholeiitic magmatism (Alto Paraná Formation, corresponding in Brazil to Serra Geral Formation; cf. Bellieni et al., 1986; Piccirillo & Melfi, 1988; Comin-Chiaramonti et al., this volume, Appendix II), both high-Ti and low-Ti, contrasting with the Nb-Ta positive spike of the spatially associated Na-alkaline magmatism (age 61-39 Ma: Comin-Chiaramonti et al., 1991).

The compositions of K-alkaline rock-types of the Asunción-Sapucai graben are distinct from those occurring in other rift-related settings, e.g. Ugandan rock-types (cf. Beccaluva et al., 1991). They scatter around the field of RRL also in the Th/Zr vs. Nb/Zr diagram (Fig. 7), and they also fall in a distinct field, intermediate between subduction-related and subduction-unrelated basal-

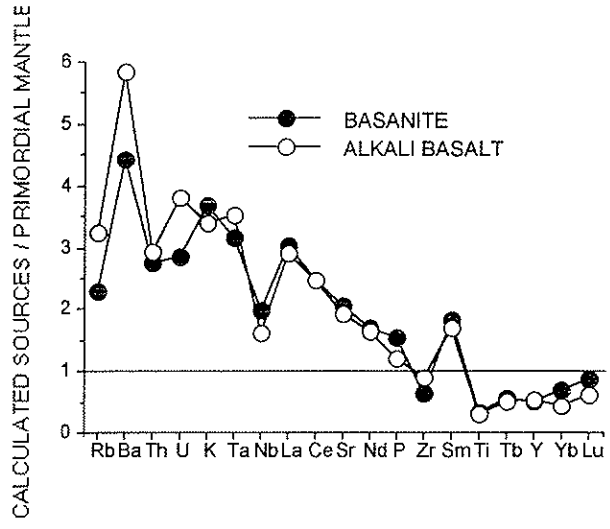

Figure 5 - Calculated concentrations of incompatible elements normalized to the primordial mantle (Sun & McDonough, 1989) in the mantle source of ASU potassic magmas.

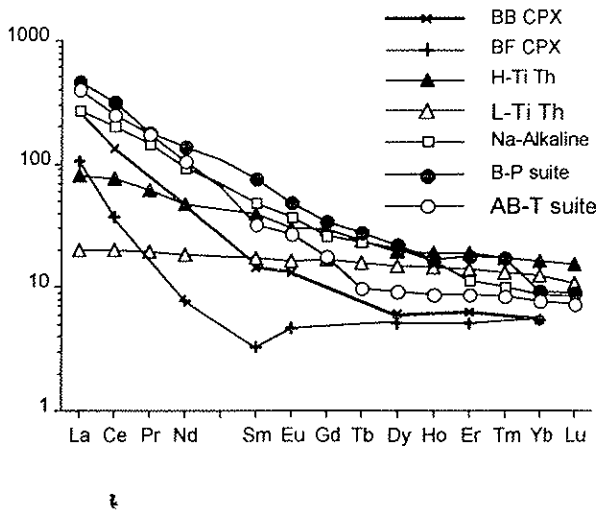

Figure 6 - Chondrite-normalized REE for ASU basaltic compositions compared with clinopyroxene from Ñemby mantle xenoliths (BB, blebs bearing; BF, bleb free: Vannucci, unpublished data; see text).

Table 6 - A. Calculated primary magmas and compositions of added minerals. Basanite, B-P suite, from basanite of Table 1, adding 23.0 % Ol + Cpx (38.6% Ol, 61.4% Cpx); alkali basalt, AB-T suite, from alkali basalt of Table 1, adding 21.5 % of Ol + Cpx (31.4% Ol, 68.6% cpx). Trace elements calculated according to Raileygh's fractionation and crystal/liquid partition coefficients as in Table 4. B. Equilibrium partial melting models (Shaw equation, according to Hanson, 1978: $C_L/C_O = 1/\{D(1-F)+F\}$, where C_L is the concentration of a given trace element in a derived melt, C_O is the composition of that element in the parent solid prior to melting, D is the bulk distribution coefficient for the mineral assemblage left in the residue, and F is the fraction of melting); data source: C, Chen, 1971; M, MacGregor, 1974; W, Wilkinson & Le Maitre, 1987. C. crystal/liquid partition coefficients (McKenzie & O'Nions, 1991 and therein references). ΣR^2: sum of the square residuals.

A

	Basanite	Alkali basalt	Olivine	Clinopyroxene
SiO_2	47.76	50.40	40.98	53.78
TiO_2	1.40	1.20		0.32
Al_2O_3	10.45	11.01		3.09
FeO_t	8.25	8.04	9.38	3.27
MnO	0.16	0.15	0.16	0.09
MgO	13.31	12.67	49.46	16.60
CaO	11.98	11.08	0.02	21.97
Na_2O	2.82	2.14		0.87
K_2O	3.42	2.95		0.01
P_2O_5	0.47	0.36		
mg#	0.74	0.76	0.90	0.90
Cr	801	674		
Ni	710	323		
Rb	45	61		
Ba	899	1147		
Th	7.5	7.9		
U	1.9	2.5		
Ta	2.4	2.6		
Nb	29	23		
La	56	53		
Ce	106	103		
Nd	48	46		
Sr	1124	1038		
Zr	121	168		
Sm	12.3	11.3		
Tb	0.64	0.58		
Y	15	16		
Yb	1.4	0.9		
Lu	0.21	0.16		

B

	Gt Per (C)	Ol (M)	Opx (M)	Cpx (M)	Gt (M)	Amph (W)		B-P 1	B-P 2	AB-T 1	AB-T 2
SiO_2	45.70	41.54	57.43	53.42	42.17	41.49	F %	3.11	3.19	3.18	3.19
TiO_2	0.10	0.02	0.28	0.49	0.30	4.79					
Al_2O_3	1.60	0.01	0.99	2.49	20.61	14.40	Ol	67.71	67.77	68.20	68.79
FeO_t	8.62	9.28	6.43	4.89	12.45	11.32	Opx	19.00	18.99	18.46	18.29
MnO	0.01	0.10	0.02	0.02	0.30	0.10	Cpx	8.70	8.69	8.71	8.69
MgO	40.97	49.00	33.62	16.79	18.50	12.49	Gt	4.52	4.54	4.15	4.22
CaO	2.53	0.03	0.94	20.86	4.46	10.67	Amph	0.07		0.47	
Na_2O	0.36		0.26	1.01	0.79	2.76					
K_2O	0.09			0.01	0.40	1.96	ΣR^2	0.039	0.040	0.042	0.043
P_2O_5	0.02					0.01					

C Partition Coefficients	Ol	Opx	Cpx	Gt	Amph	C_0	B-P 1	B-P 2	AB-T 1	AB-T 2
Rb	0.00018	0.0006	0.011	0.0007	0.3		1.46	1.49	2.10	2.02
Ba	0.0001	0.01	0.007	0.01	0.4		30.8	31.3	41.8	39.8
Th	0.0001	0.0001	0.00026	0.0001	0.001		0.23	0.24	0.25	0.25
U	0.0001	0.0001	0.00036	0.0001	0.001		0.06	0.06	0.08	0.08
K	0.0002	0.001	0.0028	0.001	1.0		919	921	905	796
Ta	0.01	0..01	0.10	0.10	0.9		0.13	0.13	0.15	0.14
Nb	0.01	0.01	0.05	0.1	0.8		1.41	1.42	1.20	1.12
La	0.0004	0.002	0.054	0.01	0.17		2.06	2.10	2.02	1.99
Ce	0.0005	0.003	0.098	0.021	0.26		4.38	4.44	4.42	4.31
Sr	0.00019	0.007	0.067	0.0011	0.12		43.0	43.8	40.9	41.0
Nd	0.0008	0.0048	0.15	0.054	0.35		2.29	2.32	2.28	2.21
P	0.043	0.014	0.009	0.19	0.20		147	146	114	113
Zr	0.01	0.03	0.1	0.155	0.35		7.09	7.16	10.08	9.85
Sm	0.0013	0.01	0.26	0.217	0.76		0.81	0.81	0.77	0.74
Ti	0.006	0.024	0.1	0.1	0.69		443	445	400	379
Tb	0.0015	0.019	0.31	0.75	0.83		0.061	0.061	0.056	0.054
Y	0.001	0.08	0.367	1.85	0.7		2.38	2.39	2.48	2.45
Yb	0.0015	0.049	0.28	4.03	0.59		0.34	0.34	0.21	0.21
Lu	0.0015	0.06	0.28	5.5	0.51		0.065	0.065	0.046	0.047

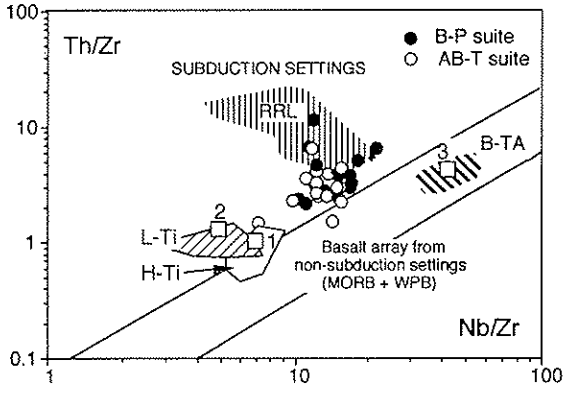

Figure 7 - 100Nb/Zr vs. 100Th/Zr ratios (after Beccaluva et al., 1991: Fig. 8, modified) showing the fitting of the selected analyses (Table 2), the fields of the Roman Region Lavas (RRL, cf. Beccaluva et al., 1991 and therein references), Toro-Ankole type-lavas (B-TA, Mitchell & Bell, 1976), tholeiitic basalts from the Paraná Basin (H-Ti and L-Ti, high- and low-titanium basalts, respectively, with $^{87}Sr/^{86}Sr$ initial isotopic ratios < 0.706; cf. Piccirillo & Melfi, 1988 and Marques et al., 1989) and the average compositions of H-Ti (1), L-Ti (2) and Na-ankaratrites (3) from central-eastern Paraguay (cf. Comin-Chiaramonti et al., this volume, Petrochemistry).

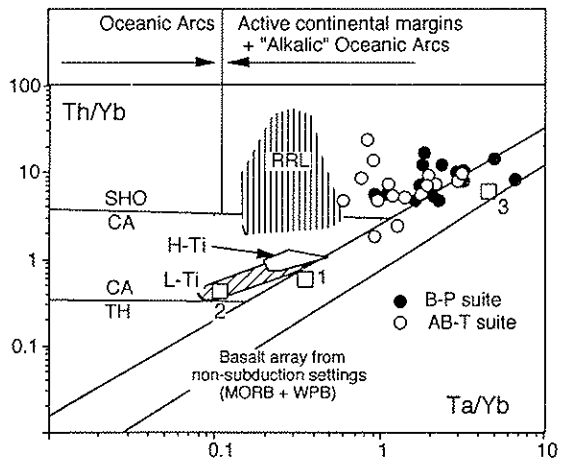

Figure 8 - Ta/Yb vs. Th/Yb diagram: Th, tholeiitic, CA, calc-alkaline, SHO, shoshonitic boundaries for arc basalts (Pearce, 1983). Other symbols as in Fig. 7.

tic compositions, in the Th/Yb vs. Ta/Yb diagram (Fig. 8). Notably, the K-alkaline rock-types from Paraguay are on trend with the tholeiitic basalts of the Serra Geral Formation, both groups being distinct from subduction-unrelated basaltic compositions. This suggests that the chemical characteristics of the K-alkaline magmatism in central-eastern Paraguay may due to a metasomatized mantle source with Nb-Ta bearing residual phases. As matter of fact, Foley & Wheller (1990) argue that melting with residual Ti-phases in the continental lithosphere will produce the same trace element spikes, and that fossil Benioff zones and former subducted slabs are not necessary for the formation of potassic-ultrapotassic rocks (cf. also Sheppard & Taylor, 1992).

The uneven rock distribution in a relatively narrow area, as central-eastern Paraguay, indicates that the subcontinental lithosphere plays an important role. Parts of the lithosphere may be

more enriched than the others, but the lithospheric control may also be of physical character: old weakness zones and bumpy lower surface would channel both migrating melts/fluids and upwelling asthenosphere repeatedly into the same region.

If this is so, we can explain also:

1) the relatively high and constant $^{87}Sr/^{86}Sr$ initial ratios (R_0, av. 0.70714±0.00024 at 128 Ma: Castorina et al., this volume, Sr/Nd) withouth intervention of crustal contamination, as shown by low $\delta^{18}O$ ‰ vs. V-SMOW of mica (+ 4.85 to + 5.54), clinopyroxene (+ 5.09 to 5.20) and whole-rocks (+5.45 to + 6.83), and by $\delta^{13}C$ ‰ vs. PDB-1 (-5.6 to -6.5) of the carbonate phases present in some magmatic rocks (cf. Castorina et al., this volume, Carbonatites);

2) the R_0 vs. measured $^{143}Nd/^{144}Nd$ variations (0.70677-0.70754 vs. 0.51159-0.51184, respectively) that show that the Early Cretaceous K-alkaline magmatism of the Asunción-Sapucaí area is related to mantle sources isotopically distinct from those of the adjoining flood basalts (age 130 Ma, R_0 = 0.70587± 0.00016: Marques et al., 1989) and from those of the Tertiary Na-magmatism of the adjoining Asunción area (age 61-39 Ma, R_0 = 0.70374± 0.00010, $^{143}Nd/^{144}Nd$ = 0.51274±0.00006), the latter having pronounced positive Ta-Nb spikes (cf. Comin-Chiaramonti et al., this volume, Petrochemistry, Fig. 16);

3) the occurrence in Eastern Paraguay of carbonatites about 130 Ma aged (both intrusive and effusive), with the same isotopic imprinting of the associated K-alkaline magmatism (Castorina et al., this volume, Carbonatites).

The high R_0 values relative to the Serra Geral tholeiites (i.e. $R_0 \geq 0.706$) were interpreted by Hawkesworth et al. (1986) as the continental extension of the Dupal anomaly, presumably subduction-related during a previous collisional event. On the contrary, Piccirillo et al. (1989, 1990) showed that the tholeiitic basalts at the central-western Paraná Basin (i.e. Eastern Paraguay) display negligible contents of any crustal component. Moreover, the emplacement of rock-types with low R_0 (≤ 0.704), as those represented by Na-alkaline magmatism in the Asunción area, would imply the existence of a very thin and limited subduction slab affecting only the potassic magma source (R_0 = 0.707).

CONCLUSIONS

1) Three main magma types are widespread in the Assunción-Sapucai (ASU) rift, the wide extensional structure at central-eastern Paraguay, i.e. tholeiitic (137-130 Ma), potassic (132-118 Ma) and sodic (61-39 Ma), all referred to various melting degrees of garnet mantle source(s).

2) ASU potassic lavas, shallow level intrusions and dykes are thought to have been derived from primary magmas with about 12-13 % MgO, generated by ~ 3% partial melting of a garnet mantle source.

3) Isotopic data and trace element indicates an enriched source. Sr-Nd systematics place the metasomatic enrichment event during the Pre-Cambrian (cf. Castorina et al., this volume, Sr/Nd). Isotopic inhomogeneities developed between the depleted matrix and enriched components, due to the different parent/daughter ratio and the latter component would predominate during the melting episode which generated the ASU potassic magmatism.

4) The primary magmas are believed to have evolved by fractionation of olivine+clinopyroxene, to produce a range of daughter products with 6-10 % MgO and characterized by phenocryst assemblage clinopyroxene+magnetite±olivine±biotite±plagioclase (B-P suite) and clinopyroxene+magnetite±plagioclase± bio-tite±alkali feldspar (AB-T suite) as phenocrysts. Post emplacement loss of K in some of the B-P products resulted in replacement of leucite by analcite, imparting a low-K character to these rocks. Phenocrystal accumulation and magma mixing were ubiquitous, resulting in complex phenocryst/xenocryst assemblages.

5) Continued fractional crystallization at low pressure may generate oversaturated trachytic liquids (AB-T suite) by amphibole removal.

6) The production of different magma-types (i.e. tholeiitic, potassic and sodic magmas) in a relatively short temporal range and in a relatively restricted area, where there are not evidences of compressional regimes, may simply reflect metasomatized lithospheric source(s) where compositional heterogeneities can be preserved, as also shown by O-C and Sr-Nd isotopic systematics and constraints.

7) The persistence of magmatism in Eastern Paraguay up to Oligocene times severely constraints the Tristan da Cunha mantle plume as interpreted by Turner et al. (1994); the presence of rock-types with $^{87}Sr/^{86}Sr$ initial ratio < 0.704 does not encourage any interpretation of Dupal anomaly inside the continent (cf. Hawkesworth et al., 1986).

ACKNOWLEDGEMENTS

Thanks are due to Brazilian (FAPESP) and Italian (CNR and MURST) agencies and to the Universities of Trieste and São Paulo for financial supports.

REFERENCES

BARTON, M. (1979) A comparative study of some minerals occurring in the K-rich alkaline rocks of the Leucite-Hills, Wyoming, the Vico vulcano, Italy, and the Toro-Ankole Region, Uganda. Neues Jb. Mineral. Abh., *137*:113-134.

BECCALUVA, L.; DI GIROLAMO, P.; SERRI, G. (1991) Petrogenesis and tectonic setting of the Roman Volcanic Province, Italy. Lithos, *26*:191-221.

BELLIENI, G.; COMIN-CHIARAMONTI, P.; MARQUES, L.S.; MARTINEZ, L.A.; MELFI, A.J.; NARDY, A.J.R.; PICCIRILLO, E.M.; STOLFA, D. (1986) Continental flood basalts from the central-western regions of the Paraná plateau (Paraguay and Argentina): petrology and petrogenetic aspects. Neues Jb. Mineral. Abh., *154*:111-139.

BITSCHENE, P.R. (1987) Mesozoicher und Känozoischer anorogener magmatismus in OstParaguay: Arbeiten zur geologie und petrologie zweier alkaliprovinzen. Ph.D. Thesis, Heidelberg University, 317p.

CAROFF, M.; MAURY, R.C; LETERRIER, J.; JORON, J.L.; COTTEN, J.; GUILLE, G. (1993) Trace element behavior in the alkali basalt-comenditic trachyte series from Mururoa Atoll, French Polynesia. Lithos, *30*:1-22.

CASTORINA, F.; CENSI, P.; BARBIERI, M.; COMIN-CHIARAMONTI, P.; CUNDARI, A.; GOMES, C.B. (this volume) Carbonatites from Eastern Paraguay: a comparison with coeval carbonatites from Brazil and Angola.

CASTORINA, F.; PETRINI, R.; COMIN-CHIARAMONTI, P.; CAPALDI, G.; PARDINI, G. (this volume) Potassic magmatism from the Asunción-Sapucai graben, Eastern Paraguay: inferences on mantle sources by Sr-Nd isotopic systematics.

CHEN, J.C. (1971) Petrology and chemistry of garnet lherzolite noduls in kimberlite from South Africa. Amer. Mineral., *56*:2098-2110.

CIVETTA, L.; FRANCALANCI, L.; MANETTI, P.; PECCERILLO, A. (1987) Petrological and geochemical variations across the Roman Comagmatic Province: inference on magma genesis and crust-mantle evolution. Accad. Lincei, *86*:250-269.

COMIN-CHIARAMONTI, P.; DEMARCHI, G.; GIRARDI, V.A.V.; PRINCIVALLE, F.; SINIGOI, S. (1986) Evidence of mantle metasomatism and heterogeneity from peridotite inclusions of Northeastern Brazil and Paraguay. Earth Planet. Sci. Lett., *77*:203-217.

COMIN-CHIARAMONTI, P.; CUNDARI, A.; GOMES, C.B.; PICCIRILLO, E.M.; BELLIENI, G.; DE MIN, A.; CENSI, P.; ORUÉ, D.; VELÁZQUEZ, V.F. (1990) Mineral chemistry and its genetic significance of major and accessory minerals from a potassic dyke swarm in the Sapucai graben, central-eastern Paraguay. Geochim. Brasil., *4*:175-206.

COMIN-CHIARAMONTI, P.; CIVETTA, L.; PETRINI, R.; PICCIRILLO, E.M.; BELLIENI, G.; CENSI, P.; BITSCHENE, P.R.; DEMARCHI, G.; DE MIN, A.; GOMES, C.B.; CASTILLO, A.M.C.; VELÁZQUEZ, J.C. (1991) Tertiary nephelinitic magmatism in Eastern Paraguay: petrology, Sr-Nd isotopes and genetic relationships with associated spinel peridotite xenoliths. Eur. J. Mineral., *3*:507-525.

COMIN-CHIARAMONTI, P.; CUNDARI, A.; GOMES, C.B.; PICCIRILLO, E.M.; CENSI, P.; DE MIN, A.; BELLIENI, G.; VELÁZQUEZ, V.F.; ORUÉ, D. (1992) Potassic dyke swarm in the Sapucai graben, Eastern Paraguay: petrographical, mineralogical and geochemical outlines. Lithos, *28:* 283-301.

COMIN-CHIARAMONTI, P.; CENSI, P.; CUNDARI, A.; GOMES, C.B.; MARZOLI, A.; PICCIRILLO, E.M. (this volume) Petrochemistry of the Early-Cretaceous potassic rocks from the Asunción-Sapucai graben, central-eastern Paraguay.

COMIN-CHIARAMONTI, P.; CUNDARI, A.; BELLIENI, G. (this volume) Mineral analyses of alkaline rock-types from the Asunción-Sapucai graben. Appendix III.

COMIN-CHIARAMONTI, P.; CUNDARI, A.; DE MIN., A; GOMES, C.B.; VELÁZQUEZ, V.F. (this volume) Magmatism in Eastern Paraguay: occurrence and petrography.

COMIN-CHIARAMONTI, P.; DE MIN, A.; GOMES, C.B. (this volume) Magmatic rock-types from the Asunción-Sapucai graben: description of the occurrences and petrographical notes. Appendix I.

COMIN-CHIARAMONTI, P.; DE MIN, A.; MARZOLI, A. (this volume) Magmatic rock-types from the Asunción-Sapucai graben: chemical analyses. Appendix II.

CUNDARI, A. & COMIN-CHIARAMONTI, P. (this volume) Mineral chemistry of alkaline rocks from the Asunción-Sapucai graben (central-eastern Paraguay).

DE MIN, A. (1993) Il magmatismo Mesozoico K-alcalino del Paraguay Orientale: aspetti petrogenetici ed implicazioni geodinamiche. Ph.D. Thesis, Trieste University, 242p.

DEMARCHI, G.; COMIN-CHIARAMONTI, P.; DE VITO, P.; SINIGOI, S.; CASTILLO, C.A.M. (1986) Lherzolite-dunite xenoliths from Eastern Paraguay: petrological contraints to mantle metasomatism. In: E.M. Piccirillo & A.J. Melfi (eds.) The Mesozoic flood volcanism from the Paraná Basin (Brazil): petrogenetic and geophysical aspects. IAG-USP, São Paulo, p.207-227.

EDGAR, A.D. (1980) Role of subduction on the genesis of leucite-bearing rocks: discussion. Contrib. Mineral. Petrol., *73*:429-431.

ERNESTO, M.; COMIN-CHIARAMONTI, P.; GOMES, C.B.; CASTILLO, A.M.C.; VELÁZQUEZ, J.C. (this volume) Paleomagnetic data from the Central Alkaline Province, Eastern Paraguay.

FOLEY, S. (1992) Petrological characterization of the source components of potassic magmas: geochemical and experimental constraints. Lithos, *28*:187-204.

FOLEY, S. & WHELLER, G.E. (1990) Parallels in the origin of the geochemical signatures of island arc volcanics and continental potassic igneous rocks: the role of residual titanates. Chem. Geol., *85*:1-18.

FREY, F.A.; GREEN, D.H.; ROY, S.D. (1978) Integrated models of basalt petrogenesis: a study of quartz tholeiites to olivine melilites from South Eastern Australia utilizing geochemical and experimental petrological data. J. Petrol., *19*:463-513.

GOMES, C.B.; COMIN-CHIARAMONTI, P.; VELÁZQUEZ, D.; ORUÉ, D. (this volume) Alkaline magmatism in Paraguay: a review.

HAMILTON, D.L. & MacKENZIE, W.S. (1965) Phase equilibrium studies in the system $NaAlSiO_4$ (nepheline) - $KAlSiO_4$ (kalsilite) - SiO_2-H_2O. Mineral. Mag., *34*:214-231.

HANSON, G.N. (1978) The application of trace elements to the petrogenesis of igneous rocks of granitic composition. Earth Planet. Sci. Lett., *38*:26-43.

HAWKESWORTH, C.J.; MANTOVANI, M.S.M.; TAYLOR, P.N.; PALACZ, Z. (1986) Evidence from the Paraná of South Brazil for a continental contribution to Dupal basalts. Nature, *322*:356-359.

LUTH, W.C. (1967) Studies in the system $KAlSiO_4$ - Mg_2SiO_4 - SiO_2 - H_2O: Part 1, Inferred phase relations and petrological applications. J. Petrol., *8*:372-416.

MacGREGOR, I.D. (1974) The system MgO-Al_2O_3-SiO_2: solubility of Al_2O_3 in enstatite for spinel and garnet peridotite compositions Amer. Mineral., *59*:110-119.

MARQUES, L.S.; PICCIRILLO, E.M.; MELFI, A.J.; COMIN-CHIARAMONTI, P.; BELLIENI, G. (1989) Distribuição de terras raras e outros elementos traços em basaltos da Bacia do Paraná (Brasil Meridional). Geochim. Brasil., *3*:33-50.

MARZOLI, A. (1991) Studio petrologico e geochimico di complessi alcalini del rift di Sapucai (Paraguay). Bs.D. Thesis, Trieste University, 201p.

McKENZIE, D.P. & O'NIONS, R.K. (1991) Partial melt distributions from inversion of Rare Earth element concentrations. J. Petrol., *32*:1021-1091.

MENZIES, M.A. & HAWKESWORTH, C.J. (1987) Mantle metasomatism. Academic Press, London, 497p.

MITCHELL, R.H. & BELL, K. (1976) Rare earth geochemistry of potassic lavas from the Birunga and Toro-Ankole regions of Uganda. Contrib. Mineral. Petrol., *58*:293-303.

O'HARA, M.J. & MATHEWS, R.E. (1981) Geochemical evolution of an advancing periodically replenished magma chamber. J. Geol. Soc. London, *138*:237-277.

PEARCE, J.A. (1983) Role of the sub-continental lithosphere in magma genesis at active continental margins. In: C.J. Hawkesworth & M.J. Norry (eds.) Continental basalts and mantle xenoliths. Shiva, Nantwitch, p.230-249.

PICCIRILLO, E.M. & MELFI, A.M. (1988) The Mesozoic flood volcanism of the Paraná Basin: petrogenetic and geophysical aspects. IAG-USP, São Paulo, 600p.

PICCIRILLO, E.M.; CIVETTA, L.; PETRINI, R.; LONGINELLI, A.; BELLIENI, G.; COMIN-CHIARAMONTI, P.; MARQUES, L.S.; MELFI, A.J. (1989) Regional variations within the Paraná flood basalts (southern Brazil): evidence for subcontinental mantle heterogeneity and crustal contamination. Chem. Geol., *75*:103-122.

PICCIRILLO, E.M.; BELLIENI, G.; CAVAZZINI, G.; COMIN-CHIARAMONTI, P.; PETRINI, R.; MELFI, A.J.; PINESE, J.J.P.; ZANTEDESCHI, P.; DE MIN, A. (1990) Lower Cretaceous dyke swarms from the Ponta Grossa Arch: petrology, Sm-Nd isotopes and genetic relationships with the Paraná flood volcanics. Chem. Geol., *89*:19-48.

ROEDER, P.L. & EMSLIE, R.F. (1970) Olivine-liquid equilibrium. Contrib. Mineral. Petrol., *29*:275-289.

SATO, H. (1977) Nickel content of basaltic magmas: identification of primary magma as a measure of the degree of olivine fractionation. Lithos, *10*:113-120.

SHEPPARD, S. & TAYLOR, W.R. (1992) Barium- and LREE-rich, olivine-mica-lamprophyres with affinities to lamproites, Mt. Bundey, northern territory, Australia. Lithos, *28*:303-326.

SCHIANO, P.; ALLEGRE, C.J.; DUPRÉ, B.; LEWIN, E.; JORON, J.L. (1993) Variability of trace elements in basaltic suites. Earth Planet. Sci. Lett., *119*:37-51.

STORMER, J.C.Jr. & NICHOLS, J. (1978) A program for interactive testing of magmatic differentiation models. Comput. Geosci., *4*: 143-159.

SUN, S-S & McDONOUGH, W.F. (1989) Chemical and isotopic systematics of oceanic basalts. In: A.D. Saunders & M.J. Norry (eds.) Magmatism in the Ocean Basins. Geol. Soc. Sp. Publ., *42*:313-345.

THOMPSON, R.N.; MORRISON, M.A.; HENDRY, G.L.; PARRY, S.J. (1984) An assessment of the relative roles of crust and mantle in magma genesis: an elemental approach. Phil. Trans. R. Soc. London, *A310*: 549-590.

TURNER, S.; REGELOUS, M.; KELLEY, S.; HAWKESWORTH, C.; MANTOVANI, M. (1994) Magmatism and continental break-up in the South Atlantic: high precision ^{40}Ar-^{39}Ar geochronology. Earth Planet. Sci. Lett., *121*:333-348.

WILKINSON, J.F.G. & LE MAITRE, R.W. (1987) Upper mantle amphiboles and micas and TiO_2, K_2O, and P_2O_5 abundances and $100Mg/(Mg+Fe^{2+})$ ratios of common basalts and andesites: implications for modal mantle metasomatism and undepleted mantle compositions. J. Petrol., *28*:37-73.

WONES, D.R. & EUGSTER, H.P. (1965) Stability of biotite: experiment, theory and application. Amer. Mineral., *50*:1228-1272.

YODER, H.S. & TILLEY, C.E. (1962) Origin of basaltic magmas: an experimental study of natural and synthetic rock system. J. Petrol., *3*:342-532.